J. Am. Chem. Soc. **1991**, *113*, 165–171 165

Stibathiolanes: Synthesis, Solid-State Structure, and Solution Behavior

Richard A. Fisher, Ralph B. Nielsen, William M. Davis, and Stephen L. Buchwald*

Contribution from the Department of Chemistry, Massachusetts Institute of Technology, Cambridge, Massachusetts 02139. *Received January 4, 1990*

Abstract: The first examples of a new class of main group metallacycles, stibathiolanes, have been synthesized via transmetalation from zirconocene metallacycles. The X-ray crystal structures of three 1-halostibathiolanes have been determined and the compounds found to be polymeric in the crystalline state. Physical and spectroscopic data indicate that the compounds are monomeric in hydrocarbon solution but that they undergo rapid-reversible halide-exchange reactions. A consequence of one of these exchange reactions is the inversion of stereochemistry at antimony. The processes have been investigated by using a variety of NMR and crossover experiments. The proposed intermediate for the inversion of stereochemistry at the metal center is supported by the solid-state structures of the compounds in which the proposed connectivity of the intermediate is crystallographically established.

Interest in organometallic compounds of the main group metals has recently grown tremendously, due in part to the wide variety of applications of these compounds in the materials sciences.[1] Despite this new activity, the synthetic strategies for main group organometallics have remained relatively undeveloped.[2] The majority of syntheses of these compounds involve classical metathesis reactions between a main group halide and an organometallic compound such as an organolithium or Grignard reagent and are limited by a lack of selectivity and by the availability of suitable organometallic precursors. The latter limitation is severe for main group metallacycles because of the paucity of suitable 1,n-dianionic (n = 3, 4, 5) reagents or their equivalents,[3] which are most often used for the synthesis of this class of molecules.[2]

In contrast, a wide variety of transition-metal metallacycles are available via methods that employ the formal reductive coupling of two unsaturated ligands as shown below.[4] A primary goal in our (and several other[5]) laboratories[6] has been the development of zirconocene-mediated reductive coupling reactions of unsaturated organic molecules and the utilization of the metallacyclic products of these reactions in organic synthesis. In a pioneering report, Fagan and Nugent recently demonstrated that zirconocene metallacycles are also extremely effective reagents for the synthesis of main group metallacycles.[7] A summary of their results is presented in Figure 1. As is evident from Figure 1, this new transformation links the synthetic power of the reductive coupling reactions of the early transition metals to the synthesis of main group metallacycles and provides a route to many new and potentially valuable classes of main group compounds.

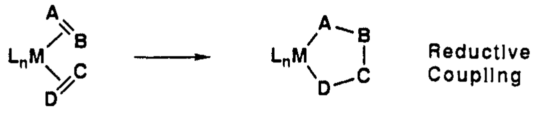

Concurrent research in our laboratories has also focused on developing and extending zirconocene-based methodology for the elaboration of main group compounds. Some of our initial efforts targeted organic heterocycles such as thiophenes[6g] and benzothioazoles,[6b] and the results of these studies are summarized in Figure 2. More recently, we have reported the synthesis and structures of a series of novel main group metallacycles, didehydrostibathiolanes, similarly obtained via transmetalation from

---

(1) (a) Bender, B. A.; Rice, R. W.; Spann, J. R. *J. Am. Ceram. Soc.* **1987**, *70*, C-58. (b) Seyferth, D.; Wiseman, G. H. *Polym. Prepr.* (*Am. Chem. Soc. Div. Polym. Chem.*) **1984**, *25*, 10. (c) Allen, S. D. In *Emergent Process Methods for High Technology Ceramics*; Davis, R. F., Palmour, H. J., III, Porter, R. L., Eds.; Plenum: New York, 1984; p 397 and other articles in this volume. (d) Schrauzer, G. N.; Prakash, H. *Solid State Commun.* **1974**, *14*, 1259. (e) Arif, A. M.; Benac, B. L.; Cowley, A. H.; Geerts, R.; Jones, R. A.; Kidd, D. B.; Power, J. M.; Schwab, S. T. *J. Chem. Soc., Chem. Commun.* **1986**, 1543. (f) Cowley, A. H.; Benac, B. L.; Ekerdrt, J. G.; Jones, R. A.; Kidd, D. B.; Lee, J. L.; Miller, J. E. *J. Am. Chem. Soc.* **1988**, *110*, 6248. (g) Theopold, K. H.; Parkanyi, L.; Byrne, E. K. *Science* **1988**, *241*, 332.

(2) For the leading references to the synthesis of main group heterocycles and metallacycles see: (a) Mathey, F.; Fisher, J.; Nelson, J. H. *Struct. Bonding* **1983**, *55*, 153. (b) Mathey, F. *Topics in Phosphorus Chemistry*; Grayson, M., Griffith, E., Eds.; Wiley: New York, 1980; Vol. 10, pp 1–128. (c) Braye, E. H.; Hubel, W.; Caplier, I. *J. Am. Chem. Soc.* **1961**, *83*, 4406. (d) Leavitt, F. C.; Manuel, T. A.; Johnson, F.; Matternas, L. U.; Lehman, D. S. *J. Am. Chem. Soc.* **1960**, *82*, 5099. (e) Dimroth, K. *Comprehensive Heterocyclic Chemistry*; Meth-Cohn, O., Ed.; Pergamon: Oxford, 1984; Vol, 1, pp 518–523. (f) Atkinson, R. E. *Comprehensive Heterocyclic Chemistry*; Meth-Cohn, O., Ed.; Pergamon: Oxford, 1984; Vol. 1, pp 544–550. (g) Armitage, D. A. *Comprehensive Heterocyclic Chemistry*; Meth-Cohn, O., Ed.; Pergamon: Oxford, 1984; Vol. 1, pp 614–617. Markl, G.; Hauptman, H.; Merz, A. *J. Organomet. Chem.* **1983**, *249*, 335.

(3) Ashe, A. J., III; Drone, F. J. *Organometallics* **1984**, *3*, 495. Buchwald, S. L.; Nielsen, R. B. *J. Am. Chem. Soc.* **1989**, *111*, 2870 and references therein.

(4) Collman, J. P.; Hegedus, L. S.; Norton, J. R.; Finke, R. G. *Principles and Applications of Organotransition Metal Chemistry*; University Science Books: Mill Valley, CA, 1987.

(5) (a) Nugent, W. A.; Calabrese, J. C. *J. Am. Chem. Soc.* **1984**, *106*, 6422. (b) Nugent, W. A.; Thorn, D. L.; Harlow, R. L. *J. Am. Chem. Soc.* **1987**, *109*, 2788. (c) Parshall, G. W.; Nugent, W. A.; Chan, D. M.-T.; Tam, W. *Pure Appl. Chem.* **1985**, *57*, 1809. (d) Negishi, E.-I.; Cederbaum, F. E.; Takahashi, T. *Tetrahedron Lett.* **1986**, *27*, 2829. (e) Negishi, E.-I.; Takahashi, T.; Seki, T.; Saburi, M.; Uchida, Y. *J. Org. Chem.* **1989**, *54*, 3521. (f) Takahashi, T.; Murakami, M.; Kunishige, M.; Saburi, M.; Uchida, Y.; Kozawa, K.; Uchida, T.; Negishi, E.-I. *Chem. Lett.* **1989**, 761. (g) Takahashi, T.; Murakami, M.; Kunishige, M.; Saburi, M.; Uchida, Y.; Negishi, E.-I. *J. Chem. Soc., Chem. Commun.* **1989**, 852. (h) Negishi, E.-I.; Holmes, S. J.; Tour, J. M.; Miller, J. A.; Cederbaum, F. E.; Swanson, D. R.; Takahashi, T. *J. Am. Chem. Soc.* **1989**, *111*, 3336. (i) Erker, G. *J. Organomet. Chem.* **1977**, *134*, 189. (j) Erker, G.; Kropp, K. *J. Am. Chem. Soc.* **1979**, *101*, 3659. (k) Erker, G.; Kropp, K. *J. Organomet. Chem.* **1980**, *194*, 45. (l) Kropp, K.; Erker, G. *Organometallics* **1982**, *1*, 1246. (m) Erker, G. *Acc. Chem. Res.* **1984**, *17*, 103. (n) Erker, G.; Czisch, P.; Mynott, R.; Tsay, Y.-H.; Krüger, C. *Organometallics* **1985**, *4*, 1310. (o) Erker, G.; Dorf, U.; Mynott, R.; Tsay, Y.-H.; Krüger, C. *Angew. Chem.* **1985**, *97*, 572. (p) Erker, G.; Krüger, C.; Müller, G. *Adv. Organomet. Chem.* **1985**, *24*, 1. (q) Erker, G.; Mühlenbernd, T.; Benn, R.; Rufinska, A.; Tainturier, G.; Gautheron, B. *Organometallics* **1986**, *5*, 1023. (r) Erker, G.; Sonsna, F.; Zwettler, R.; Krüger, C. *Organometallics* **1989**, *8*, 451.

(6) (a) Buchwald, S. L.; Watson, B. T.; Huffman, J. C. *J. Am. Chem. Soc.* **1986**, *108*, 7411. (b) Buchwald, S. L.; Watson, B. T.; Lum, R. T.; Nugent, W. A. *J. Am. Chem. Soc.* **1987**, *109*, 7137. (c) Buchwald, S. L.; Sayers, A.; Watson, B. T. *Tetrahedron Lett.* **1987**, *28*, 3245. (d) Buchwald, S. L.; Nielsen, R. B. *Chem. Rev.* **1988**, *88*, 1047. (e) Buchwald, S. L.; Wannamaker, M. W.; Watson, B. T.; Dewan, J. C. *J. Am. Chem. Soc.* **1989**, *111*, 4486. (f) Buchwald, S. L.; Fang, Q. *J. Org. Chem.* **1989**, *54*, 2793. (g) Buchwald, S. L.; Nielsen, R. B. *J. Am. Chem. Soc.* **1989**, *111*, 2870. (h) Buchwald, S. L.; Nielsen, R. B.; Dewan, J. C. *J. Am. Chem. Soc.* **1987**, *109*, 1590. (i) Buchwald, S. L.; Lum, R. T.; Fisher, R. A.; Davis, W. M. *J. Am. Chem. Soc.* **1989**, *111*, 9113.

(7) (a) Fagan, P. J.; Nugent, W. A. *J. Am. Chem. Soc.* **1988**, *110*, 2310. See also: (b) Fagan, P. J.; Burns, E. G.; Calabrese, J. C. *J. Am. Chem. Soc.* **1988**, *110*, 2979.

0002-7863/91/1513-165$02.50/0 © 1991 American Chemical Society

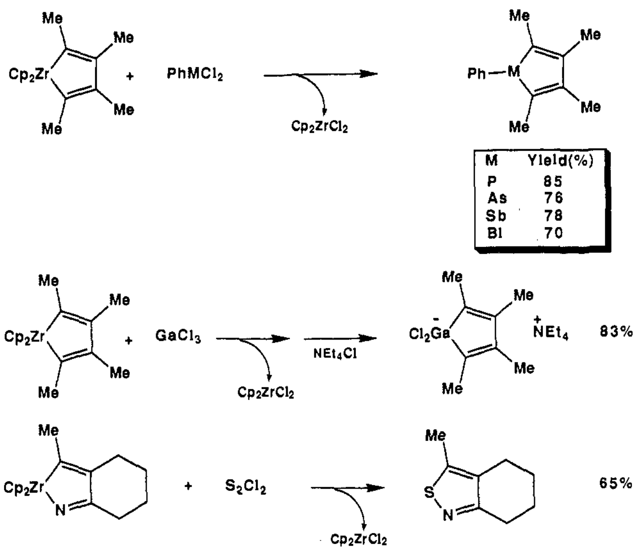

M	Yield(%)
P	85
As	76
Sb	78
Bi	70

Figure 1.

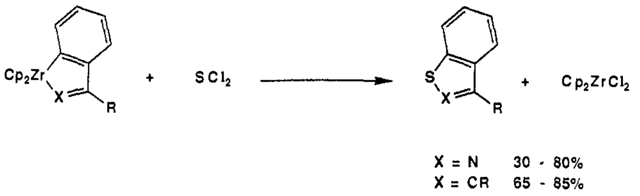

X = N 30 - 80%
X = CR 65 - 85%

Figure 2.

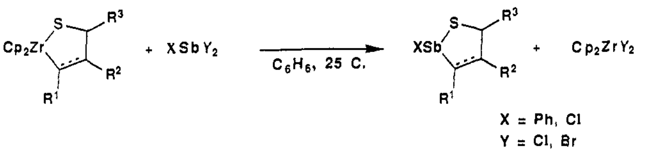

X = Ph, Cl
Y = Cl, Br

Figure 3.

zirconium precursors.[8] In this paper we wish to report the scope of this transformation and describe in more detail the solid-state structures and unusual solution behavior of the 1-halostibathiolanes.

Results and Discussion

The stibathiolanes and their didehydro analogues were synthesized as shown in Figure 3. As reported previously, zirconocene metallacycles undergo clean transmetalation reactions with a variety of main group di- and trihalides. Thus, treatment of the zirconacycle with 1 equiv of $XSbY_2$ (X = Cl, Br, Ph; Y = Cl, Br) results in the rapid and quantitative formation of the corresponding stibacycle and zirconocene dihalide. Removal of the solvent in vacuo, extraction with hexanes, and flash chromatography on alumina(III) allows for the ready isolation of the 1-phenyl stibacycles. The 1-halo metallacycles are decomposed by alumina(III), but they may be purified in good yield by chromatography on anhydrous $MgSO_4$. The results for the disubstituted metallacycles (R^3 = H in Figure 3) are summarized in Figure 4.

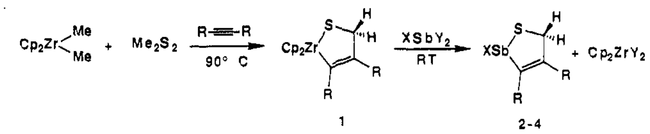

1	R
1a	R = H
b	R = Me
c	R = Ph

	X	R	Yield (%)
2a	X = Ph	R = H	86
2b	X = Cl	R = H	100*
3a	X = Ph	R = Me	84
3b	X = Cl	R = Me	80
3c	X = Br	R = Me	90
4a	X = Ph	R = Ph	85
4b	X = Cl	R = Ph	80
4c	X = Br	R = Ph	83

Figure 4. All yields refer to isolated product except for compound **2b** which cannot be separated from Cp_2ZrCl_2; the yield for this entry was determined by ^1H NMR analysis of the reaction mixture.

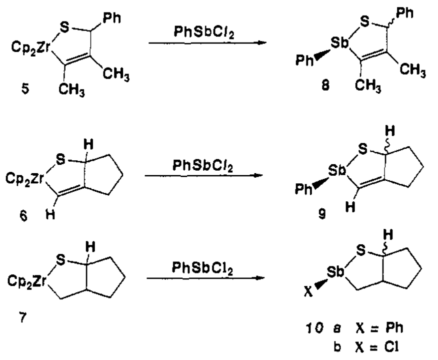

	Yield (%)	Diastereomeric Ratio
8	66	55 : 45
9	69	85 : 15
10	a 61 b 58	Only one Diastereomer detected

Figure 5. All yields refer to isolated product. Diastereomeric ratios were determined by ^1H NMR analysis of the crude reaction mixtures.

Incorporation of a third substituent into the metallacycle ($R^3 \neq$ H) generates a second stereogenic center in the ring and thereby the possibility of forming diastereomers. Our studies indicate that with simple alkyl and aryl substituents, little or no diastereoselectivity is observed on transmetalation from zirconium to antimony. For example, when a benzene solution of compound **5** is treated with $PhSbCl_2$, a 55:45 mixture of diastereomers of **8** is produced. In all cases the presence of two diastereomers is readily discernable from the ^1H and ^{13}C NMR spectra. Diastereomeric mixtures of **8** may be enriched in the major component by repeated fractional recrystallization, but complete separation cannot be accomplished. When mixtures of **8**, thus enriched in the major component, are heated to 80 °C, no interconversion of diastereomers is observed (by ^1H NMR). The diastereoselectivity of the reaction may be increased substantially only by constraining the third substituent to lie within a fused five-membered ring (see Figure 5). The diastereomers of **9** are again only partially separable by repeated recrystallizations and, as with **8**, stable to interconversion at 80 °C. In contrast, compounds **10a** and **10b** are each obtained as a single diastereomer. Heating benzene solutions of **10a** or **10b** to 80 °C does not convert either to detectable amounts of their diastereomers. The solid-state structure of **10b** has been determined, and, as will be discussed, the stereochemical relationship between the chlorine atom and the fused five-membered ring was found to be cis. Available spectroscopic data are insufficient to assign the relative stereochemistry of the preferred diastereomers of **8**, **9**, or **10b**.

Solid-State Structures of the 1-Halo-Substituted Stibacycles. The X-ray crystal structures of compounds **3b** and **4c** were previously reported;[8] the features relevant to this paper are reproduced in Figures 6 and 7. Both compounds are polymeric in the crystalline state.[9] The structures consist of a single stibacycle per asymmetric unit cell. However, the antimony and sulfur atoms of the molecule are mutually bound to the sulfur and antimony atoms of a neighboring molecule (contact distance ca. 3.1 Å), effecting a see-saw geometry about the antimony atoms of the dimeric unit. The sulfur atom of each stibacycle is puckered out of the plane (ca. 0.26 Å) of the metallacycles in the direction of the second antimony atom to which it is bound. Additional close contacts between the antimony atoms and heteroatoms of neighboring molecules give rise to an interconnecting network of antimony, sulfur, and halogen atoms. Each antimony atom is asymmetrically bridged by two halogen atoms (long contacts

---

[8] (a) Buchwald, S. L.; Fisher, R. A.; Davis, W. M. *Organometallics* **1989**, *8*, 2082. Two reports on the use of titanocene metallacycles for the synthesis of phospha-[8bc] and arsacyclobutenes[8c] have recently appeared. (b) Doxsee, K. M.; Shen, G. S.; Knobler, C. B. *J. Am. Chem. Soc.* **1989**, *111*, 9129. (c) Tumas, W.; Suriano, J. A.; Harlow, R. L. *Angew. Chem., Int. Ed. Engl.* **1990**, *29*, 75.

[9] The polymeric nature of compound **4c** was not previously reported.

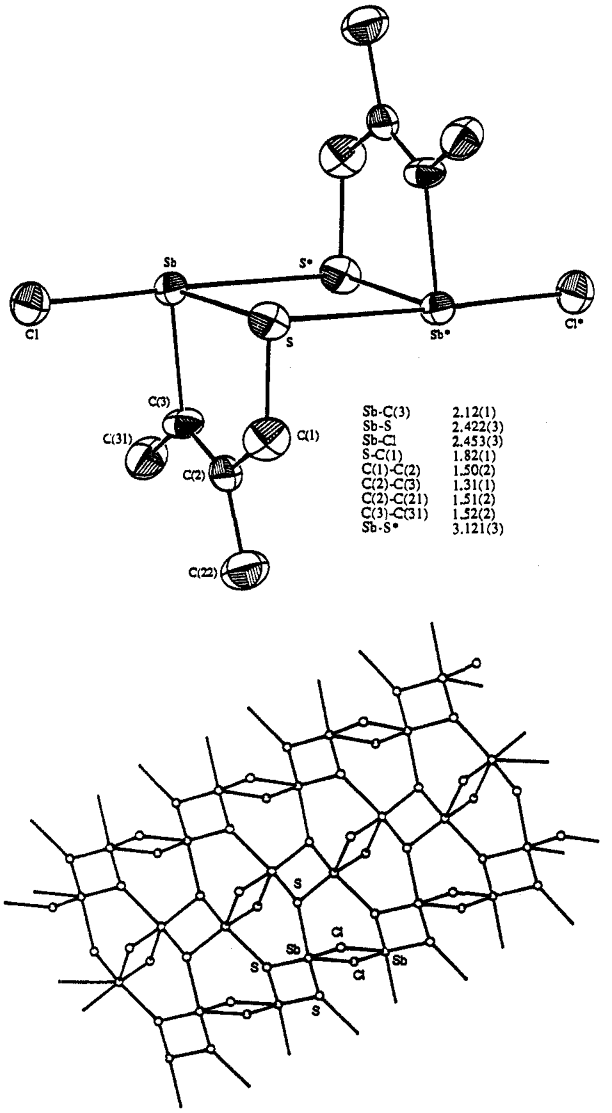

Figure 6. (a, top) The dimeric unit of **3b** with selected bond lengths. (b, bottom) The lattice of interconnecting Sb, S, Cl atoms viewed along the ac plane. Carbon atoms are omitted for clarity.

3.785(3) for **3b**; 3.986(1) for **4c**) to an antimony atom of another dimeric unit. The resulting chain of antimony atoms, bridged alternately by halogen and sulfur atoms, propagates through the unit cell. Compound **3b** contains an additional antimony–sulfur contact (ca. 3.1 Å) which cross-links adjacent strands of the polymeric structure generating a puckered net of antimony–sulfur parallelograms propagating through the ac plane of the unit cell.

A determination of the molecular structure of compound **10b** was undertaken to determine the relative stereochemistry in the molecule, as well as to establish the generality of the polymeric nature of the halostibathiolanes. As with the cases of the less substituted analogues, **10b** is polymeric in the crystalline state; however, the structure of the monomer differs markedly from those of **3b** and **4c** (see Figure 8). The saturated [3.0.3] ring system is highly puckered. Each of the five-membered rings is composed of four nearly planar atoms and C(5) which is greater than 0.5 Å out of either plane. The five-membered ring containing the heteroatoms also exhibits a slight twist; C(1) and C(6) are displaced slightly (0.13 and 0.12 Å, respectively), and in opposite directions, from the plane defined by Sb, S, C(1), and C(6). The polymeric structure of **10b** is very similar to those of **3b** and **4c**. The antimony and sulfur atoms in each asymmetric unit are mutually bound to the sulfur and antimony atoms of a neighboring molecule, again effecting a see-saw geometry about the antimony atoms of the dimeric unit. The intermolecular Sb–S bond distances of the dimeric unit are in good agreement with those of **3b** and **4c**. As in **3b**, the antimony atoms are bridged asymmetrically by chlorine atoms with a long contact of 3.44 Å; however, unlike **3b**, no cross-linking of adjacent polymer chains occurs. A view of the crystal lattice is shown in Figure 8c; additional details of the structure and its determination may be found in the Experimental Section.

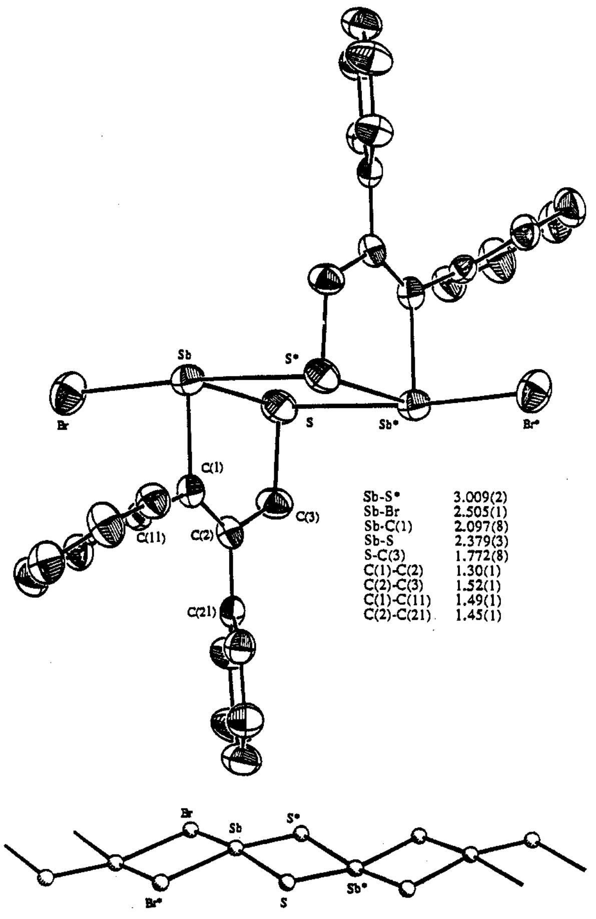

Figure 7. (a, top) The dimeric unit of **4c** with selected bond lengths. (b, bottom) Chains of Sb atoms bound alternately by S and Br atoms, carbon atoms omitted for clarity, viewed down the *c* axis.

Solution Behavior. During the course of our investigations, we observed some unusual spectroscopic behavior for the halo-substituted metallacycles. These observations, coupled with the established tendency of these molecules to aggregate in the solid state, prompted us to probe the nature of the spectroscopic anomalies. Solution molecular weight determinations indicate that the compounds are monomeric in benzene solution.[10] The ^1H NMR spectra of the 1-phenyl-substituted metallacycles exhibit a pair of well-resolved doublets for the diastereotopic methylene protons, independent of temperature or concentration. In contrast, the diastereotopic protons of the 1-halo-substituted stibacycles undergo a concentration-dependent exchange reaction. Under appropriate conditions of dilution or low temperature, the diastereotopic protons appear as well-resolved doublets, very similar in nature to the spectra of the phenylstibacycles. The spectra of **3b** are representative and are shown in Figure 9 as a function of temperature and concentration. The increase in the rate of exchange observed with increased concentration indicates the reaction is greater than first order in stibacycle. A more detailed analysis of the line shapes is prevented because the signal for the two protons is not well behaved as it approaches the fast exchange limit. After coalescence, the signal sharpens with increased temperature (or concentration) to a line width of ca. 50 Hz, but does not sharpen further under any conditions. While the reasons for this behavior are not entirely clear, it appears that more than a single process is responsible for the dynamic nature of the ^1H NMR spectra of these molecules.

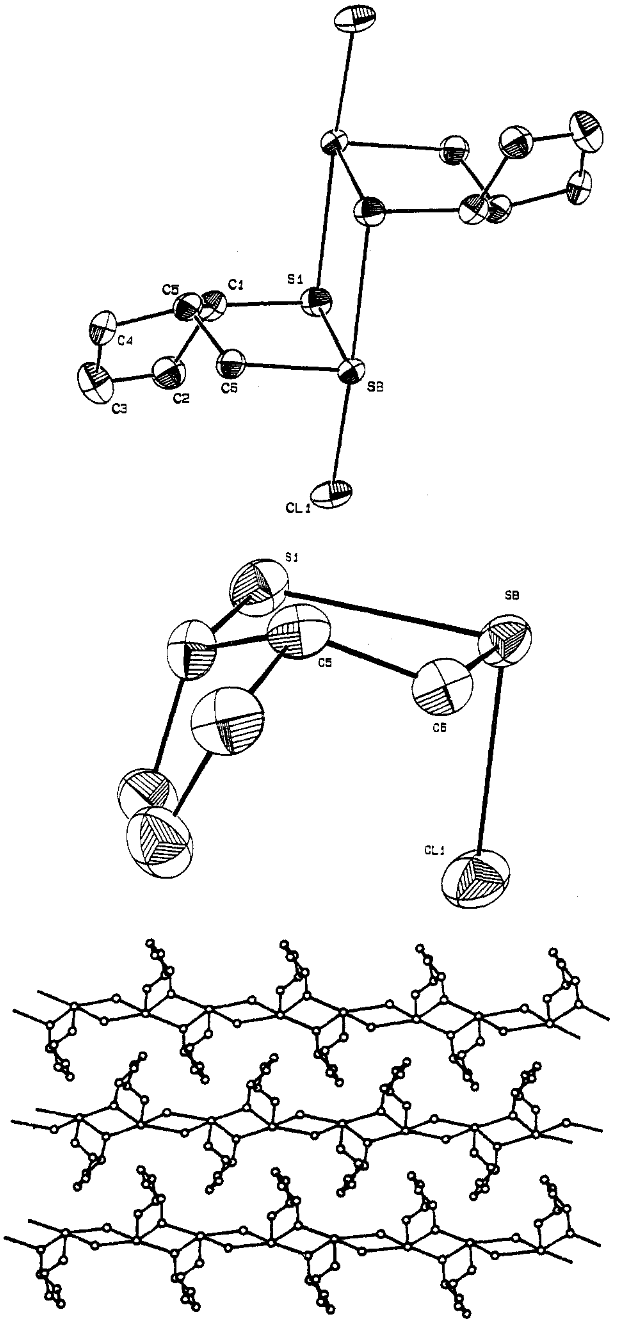

Figure 8. (a, top) The dimeric unit of **10b** with selected bond lengths. (b, middle) View of the monomer showing the puckered [3.0.3] ring system. (c, bottom) The polymeric structure of **10b**, viewed down the *a* axis of the unit cell.

An attractive explanation for the fluxional behavior of the diastereotopic methylene protons is the degenerate exchange of halide atoms via an intermediate in which the methylene protons are spectroscopically equivalent.[11] In order to establish whether such an exchange was occurring, a series of crossover experiments were conducted. The experiments involved the mixing of, for example, compounds **3c** and **4b** under various reaction conditions and analyzing for the formation of the crossover products **3b** and **4c**. Initial attempts at analyzing for crossover products by ^{13}C NMR spectroscopy were frustrated by the virtually identical chemical shifts of the chloro- and bromo-substituted metallacycles. This situation was further complicated by the realization that a rapid halide exchange, if it were occurring, could render the interpretation of the ^{13}C spectra extremely difficult. Furthermore, unambiguous assignment of resonances due to the crossover products could not be made for solutions of authentic mixtures of the four compounds. Mass spectroscopy was found to be a more successful method of analyzing for the formation of crossover products. When equimolar amounts of compounds **3c** and **4b** were dissolved in benzene, ether, or THF, the solvent subsequently removed in vacuo, and the solid residue was analyzed by mass spectrometry, all four compounds (**3b**,**c**, **4b**,**c**) were found to be present in nearly equal amounts. Control reactions were performed to ensure that the compounds were not undergoing exchange either upon standing as solids or within the mass spectrometer. For instance, when compounds **3c** and **4b** were mixed together as solids and analyzed under the same experimental conditions used for the crossover experiments, less than 10% crossover occurred. The amount of crossover products detected was not a function of the time the solid mixtures, from either the crossover experiments or the control reactions, were allowed to stand before analysis.

These findings firmly establish that a rapid exchange of halide atoms is occurring in solutions of the 1-halo-substituted stibathiolanes. The equilibration of the methylene protons, as observed in the ^{1}H NMR spectra, and the previously discussed crystal structures suggest that the halide exchange may occur through a bridging intermediate in which the methylene protons are enantiotopic. A structure meeting these requirements is shown in Figure 11. The exchange of halide atoms through an intermediate containing a σ plane of symmetry, such as A, would result in the inversion of stereochemistry at the metal and account for the observed equilibration of methylene protons.

Other mechanisms can be imagined for the exchange of halide atoms and the inversion of stereochemistry at antimony. For example, homolytic or heterolytic cleavage of the Sb–Cl bond followed by recombination with the halide radical or anion would account for these results. While the dependence of the rate of the reaction on the concentration of the stibacycle (as discussed, the reaction is approximately second order in stibacycle) renders these possibilities unlikely, we have not been able to rigorously eliminate radical or ionic mechanisms for the exchange. However, several additional facts further diminish the likelihood that exchange of halide atoms occurs via radical or anionic intermediates. Neither heterolytic nor homolytic cleavage of antimony(III)–chlorine bonds under the mild conditions we observe exchange is, to the best of our knowledge, precedented. The exchange reaction does not display significant dependence on solvent polarity as would be anticipated for an ionic reaction. The halostibacycles do not exchange halides with alkyl bromides (1-bromobutane or 5-bromo-1-pentene). The rate of the exchange reaction is unaffected either by the presence of these alkyl bromides (0.1 to 5.0 equiv) or by the presence of oxygen.

Final Considerations and Conclusions. The rapid inversion of stereochemistry in solutions of the halostibacycles necessitates a careful evaluation of the relative stereochemistry of compound **10b**. As discussed previously, and as shown in Figure 8, the diastereomer observed in the solid-state structure contains the chlorine atom and the two carbon substituents (the fused 5-membered ring) on a single face of the metallacycle. Although the compound appears to exist as a single diastereomer in solution, it is possible, and in fact likely given the solution behavior of **3bc** and **4bc**, that **10b** exists in solution as an equilibrium of two diastereomers, with one of the two being greatly favored over the other. While the relative stereochemistry of the preferred diastereomer in solution may be the same as that in the solid state, we have refrained from assigning the stereochemistry in solution as cis because of a lack of supporting spectroscopic evidence.

---

(10) (a) Compounds **2a**, **3a**,**b**, and **4c** were subjected to solution molecular weight determinations as described elsewhere.[9b] The concentration range for the molecular weight determinations was 0.0560–0.1700 M. (b) Bercaw, J. E.; Burger, B. J. Vacuum Line Techniques for Handling Air-Sensitive Organometallic Compounds. In *Experimental Organometallic Chemistry: A Practicum in Synthesis and Characterization*; Wayda, A. L., Darensbourg, M. Y., Eds.; ACS Symp. Ser. 357; American Chemical Society; Washington, DC, 1987; pp 79–102.

(11) Halide exchange reactions are ubiquitous for the main group elements. See for example: Cotton, F. A.; Wilkinson, G. *Advanced Inorganic Chemistry*, 5th ed.; Wiley: New York, 1988; pp 11–213, 391–396. (b) Doak, G. O.; Freedman, L. D. *Organometallic Compounds of Arsenic, Antimony, and Bismuth*; Wiley: New York, 1970.

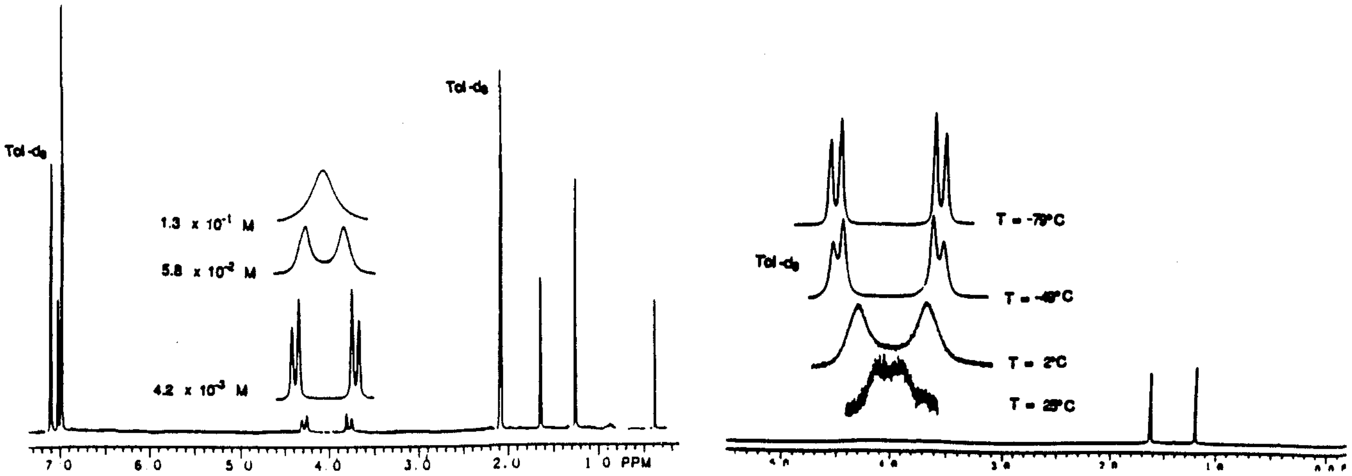

Figure 9. ^{1}H NMR of **3b** as a function of temperature (a, left) and concentration (b, right). The lowest trace in part b is for an equimolar C_6D_6 sample.

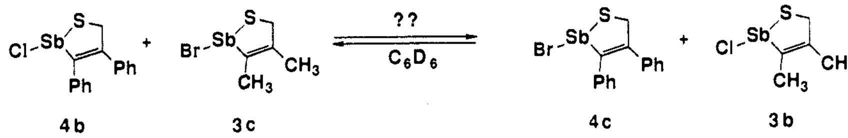

Figure 10.

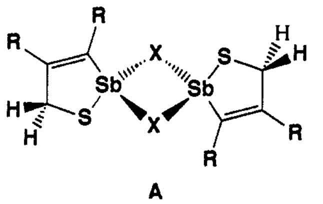

A

Figure 11.

In summary, we have successfully applied a transmetalation strategy to the synthesis of a number of representatives of a new class of main group metallacycle. The solid-state structures of three of these compounds have been determined and in all cases the compounds are polymeric in the crystalline state. We have investigated the unusual NMR behavior of these compounds by a variety of NMR and crossover experiments and have determined that a halide exchange is occurring in solutions of these species. The proposed mechanism for the exchange reaction is sufficient to explain the observed NMR behavior and the connectivity of the proposed intermediate has been crystallographically established in all three of the solid-state structures.

Experimental Section

General. All reactions were conducted under an atmosphere of argon with standard Schlenk techniques or under a nitrogen atmosphere in a Vacuum Atmospheres Co. drybox. Nuclear magnetic resonance (NMR) spectra were recorded on a Bruker WM-250, Varian XL-300, Varian Gemini 300, Varian XL-400, or Varian VXR-500 Fourier transform spectrometer. Infrared (IR) spectra were recorded on a Mattson Cygnus Starlab 100 Fourier transform spectrometer. Gas chromatography analyses were performed on a Hewlett Packard Model 5890 G with a 3392A integrater and FID detector using a 25-m capillary column with cross-linked SE-30 as a stationary phase. Electron impact mass spectra and high-resolution mass determinations (HRMS) were recorded on a Finnegan MAT System 8200. Melting points were measured on a Haake Buchler melting point apparatus and are uncorrected. Elemental analyses were performed by Desert Analytics, Tucson, AZ.

Tetrahydrofuran, benzene, and diethyl ether were dried and deoxygenated by refluxing over sodium-benzophenone ketyl followed by distillation. Hexane was deolefinated by stirring over H_2SO_4, from which it was decanted and then stored over CaH_2. The deolefinated hexane thus obtained was dried and deoxygenated by refluxing over sodium-benzophenone ketyl followed by distillation. Cp_2ZrCl_2 was purchased from Boulder Scientific Inc., Mead, CO. $SbCl_3$ and Ph_3Sb were purchased from Strem Chemicals Inc., Newburyport, MA. All other reagents either were prepared according to published procedures or were available from commercial sources and used without further purification. Note: The syntheses of the stibole derivatives described in this paper were performed under an inert atmosphere because of the sensitivity of the zirconium starting materials. Once the transmetalation reaction is complete, the removal of solvent and subsequent purifications may be performed in air without deleterious effects. The compounds are best stored under a dry atmosphere of nitrogen or argon.

Synthesis and Characterization of Compounds. Compounds **1–4** were prepared as previously described.[8a] The zirconium metallacycles **5–7** were prepared as follows.

Compound 5. Cp_2ZrMe_2 (5.03 g, 20 mmol), benzene (15 mL), 2-butyne (3 mL, 37 mmol), and benzyl mercaptan (2.35 mL, 20 mmol) were combined in a glass pressure vessel at 0 °C, and the stirred solution was allowed to slowly warm to room temperature. When methane evolution ceased, the vessel was again cooled to 0 °C and vented briefly to reduce the pressure. The mixture was stirred and heated to 95 °C for 4 h. During the reaction, some yellow solid precipitated. The mixture was cooled to room temperature and vented and hexane (50 mL) was added. The mixture was cooled to 0 °C, the supernatant was decanted, and the solid product **5** was washed with 2 X 10 mL of hexane at 0 °C and vacuum dried. Yield 7.50 g (94%). ^{1}H NMR (500 MHz, C_6D_6) showed a 6:4 ratio of two compounds, each consistent with the formulation. Major component: δ 1.59 (s, 3 H), 1.77 (s, 3 H, overlapped), 4.61 (s, 1 H), 5.48 (s, 5 H), 5.95 (s, 5 H), 6.9-7.6 (m, 5 H, overlapped). Minor component: δ 1.56 (s, 3 H), 1.77 (s, 3 H, overlapped), 4.58 (s, 1 H), 5.41 (s, 5 H), 5.95 (s, 5 H), 6.9-7.6 (m, 5 H, overlapped). $^{13}C\{^1H\}$ NMR of both components (125.7 MHz, C_6D_6) δ 18.56, 18.77, 26.26, 26.51, 69.73, 70.81, 108.72, 108.96, 109.36, 109.54, 126.95, 127.06, 127.18, 127.27 (other aryl signals obscured by solvent), 140.48, 141.50, 146.64, 147.02, 176.85, 177.47. IR (KBr) 3023, 2955, 2852, 2838, 1595, 1483, 1450, 1366, 1072, 1020, 794, 736, 699, 642, 589, 514, 425 cm^{-1}. Anal. Calcd for $C_{21}H_{22}SZr$: C, 63.43; H, 5.58. Found: C, 63.58; H, 5.75. A further discussion of this and related species may be found elsewhere.[6h]

Compound 6. In a glass pressure vessel at 0 °C were combined Cp_2ZrMe_2 (2.515 g, 10 mmol, preparation given below), benzene (20 mL), and the 5-hexene-1-thiol (1.16 g, 10 mmol). The solution was stirred at 0 °C to room temperature for 3 h and was then heated to 90 °C for 17 h. Solid precipitated during the reaction. The vessel was cooled to room temperature and vented. Hexane (30 mL) was added, the supernatant was decanted, and the solid product was washed with 4 X 20 mL of hexane and vacuum dried. Yield 1.808 g (54%) as a yellow powder. ^{1}H NMR (300 MHz, C_6D_6) showed a fluxional spectrum due to dimer formation, with alkyl signals δ 0.5–2.1 and 2.6–3.1 (total of 10 H), and four Cp signals in ca. 3:1:1:3 ratio, d 5.64, 5.66, 5.70, 5.72 (total of 10 H). Because of limited solubility, no ^{13}C NMR spectrum was obtained. IR (KBr) 2946, 2940, 2863, 1439, 1435, 1365, 1233, 1018, 1012, 844, 794 cm^{-1}. Anal. Calcd for $C_{16}H_{20}SZr$: C, 57.26; H, 6.01. Found: C, 57.24, H, 6.00.

Compound 7. Compound **7** was prepared by the same procedure as **6**, using the 5-hexyne-1-thiol (1.23 g, 10 mmol, preparation given below). The product was washed with hexane at 0 °C. Yield 2.25 g (67%) after drying, as a very sparingly soluble powder. ^{1}H NMR (400 MHz, C_6D_6) showed some broadening of peaks due to dimer formation, but the coalescence temperature appears to be below room temperature. δ 0.86 (m, 1 H), 1.62 (m, 1 H), 1.82 (m, 1 H), 2.05 (m, 1 H), 2.30, 2.48 (ab of multiplets, 2 H), 3.80 (m, 1 H), 5.75 (s, 5 H), 5.80 (s, 5 H), 6.30 (m, 1 H). No ^{13}C NMR spectrum could be obtained. IR (KBr) 2941, 2890, 1592, 1587, 1439, 1012, 792, 727 cm^{-1}. Anal. Calcd for $C_{16}H_{18}SZr$: C, 57.61; H, 5.44. Found: C, 57.63; H, 5.56.

Preparation of 5-Hexene-1-thiol. A mixture of 1-bromo-5-hexene (4.08 g, 25 mmol), thiourea (1.91 g, 25 mmol), and ethanol (15 mL) was refluxed for 16 h. The solvent was evaporated to give a viscous oil. The oil was dissolved in 20 mL of water, with 5 mg of hydroquinone was added as an inhibitor. A solution of 2 g of NaOH in 10 mL of water was added, and the resulting two-phase mixture was stirred for 10 min at room temperature and poured into a separatory funnel with 50 mL of water and 50 mL of pentane. The mixture was acidified with 15% H_2SO_4. The organic layer was dried over $MgSO_4$ and evaporated to yield 5-hexene-1-thiol as a clear oil, which was pure by GC and NMR. Yield 2.06 g (71%). ^{1}H NMR (300 MHz, $CDCl_3$) δ 1.33 (t, J = 7 Hz, 1 H), 1.49 (m, 2 H), 1.52 (m, 2 H), 2.06 (m, 2 H), 2.53 (m, 2 H), 5.0 (m, 2 H), 5.80 (m, 1 H). $^{13}C\{^1H\}$ NMR (75.4 MHz, $CDCl_3$) δ 24.44, 27.54, 33.13, 33.41, 114.68, 138.42.

Preparation of 5-Hexyne-1-thiol. The *p*-toluenesulfonate of 5-hexyn-1-ol (50 mmol) was prepared with use of conventional procedures. This was combined with thiourea (3.80 g, 50 mmol) in ethanol (30 mL), and the mixture was refluxed for 4 h. Evaporation of the solvent gave an oil that was slurried with 30 mL of water. A solution of 4 g of NaOH in 30 mL of water was added, followed by 100 mL of pentane. The mixture was stirred for 1 h at room temperature and acidified with 15% H_2SO_4. The organic layer was evaporated to give 5-hexyne-1-thiol as an oil (4.82 g, 84%). GC showed 8% of the disulfide as an impurity. ^{1}H NMR (400 MHz, $CDCl_3$) δ 1.37 (t, J = 7 Hz, 1 H), 1.6–1.8 (m, 4 H), 1.96 (m, 1 H), 2.12 (m, 2 H), 2.55 (m, 2 H). $^{13}C\{^1H\}$ NMR (75.4 MHz, $CDCl_3$) (multiplicity from gated decoupling) δ 17.91 (t), 24.07 (t), 27.00 (t), 32.86 (t), 68.60 (d), 83.94 (s).

Preparation of 1-Phenylstibacycles. The zirconacycle (1.50 mmol) was slurried in 10 mL of benzene in the drybox. Phenylantimony dichloride (0.404 g, 1.50 mmol) was added all at once as a solid. After 5 min, the Schlenk flask was sealed with a septum and brought out of the drybox, and the solvent was removed, in vacuo, on a Schlenk line. Zirconocene dichloride and the desired antimony metallacycle were the only species detectable by ^{1}H NMR in the crude reaction mixture. The solid residue was extracted with 10/1 hexanes–ether and rapidly chromatographed on alumina III.

Compound 8. On removal of the solvent, **8** was obtained as a white solid. Yield 0.371 g, 0.99 mmol, 66%. Recrystallization was most successfully accomplished from 10% hexane in toluene solution. ^{1}H NMR (300 MHz, C_6D_6) (the major diastereomer in recrystallized samples) δ 7.71 (d, J = 4.5 Hz, 2 H), 7.3–6.98 (m, 10 H), 5.75 (br s, 1 H), 1.65 (s, 3 H), 1.32 (s, 3 H). $^{13}C\{^1H\}$ NMR (75.4 MHz, $CDCl_3$) (as a mixture of diastereomers) δ 149.8, 149.0, 144.5, 144.3, 142.4, 138.1, 137.4, 134.1, 128.5, 127.3, 126.9, 126.8, 68.66, 68.61, 18.54, 18.34, 17.73, 17.46. Anal. Calcd for $C_{17}H_{17}SSb$: C, 54.43; H, 4.57. Found: C, 54.79, H, 4.50.

Compound 9. On removal of the solvent, the product was obtained as a white solid. Yield 0.321 g, 1.03 mmol, 69%. ^{1}H NMR (300 MHz, C_6D_6) (resonances of major diasteroemer given where possible) δ 7.55 (dd, J = 6.25, 2.0 Hz, 2 H), 7.10 (m, 3 H), 6.10 (s, 1 H), 4.61 (m, 1 H), 1.95–1.5 (overlapping multiplets, ~9 H, methylene protons of both diastereomers). $^{13}C\{^1H\}$ NMR (75.4 MHz, $CDCl_3$) δ 135.06, 134.24, 128.88, 128.74, 128.70, 119.54, 63.60, 34.30, 29.77, 29.76. Anal. Calcd for $C_{12}H_{13}SSb$: C, 46.34; H, 4.21. Found: C, 46.33, H 4.16.

Compound 10a. On removal of the solvent, the product was obtained as a white solid. Yield 0.284 g, 0.92 mmol, 61%. Mp 136–138 °C. ^{1}H NMR (300 MHz, C_6D_6) δ 7.59 (d, 2 H), 7.16 (m, 3 H), 3.76 (m, 1 H), 2.81 (m, 1 H), 1.95–1.88 (overlapping multiplets, 3 H), 1.75 (m, 2 H), 1.3 (m, 3 H). $^{13}C\{^1H\}$ NMR (75.4 MHz, $CDCl_3$) δ 141.4, 134.4, 129.9, 128.6, 60.69, 53.44, 34.69, 33.14, 31.49, 22.97. Anal. Calcd for $C_{12}H_{12}SSb$: C, 46.49; H, 3.90. Found: C, 46.95, H, 4.11.

Preparation of 1-Halostibacycles. The zirconacycle (1.50 mmol) was slurried in 10 mL of benzene in the drybox. Antimony trichloride (0.342 g, 1.50 mmol) was added all at once as a solid. After 5 min, the Schlenk flask was sealed with a septum and brought out of the drybox, and the solvent was removed, in vacuo, on a Schlenk line. The zirconocene dichloride was separated from the product by extraction with 10/1 hexanes–ether followed by rapid chromatography on anhydrous $MgSO_4$. Note: The chemical shifts of the halo-substituted metallacycles show a marked dependence on solvent and concentration.

Table I. Fractional Atomic Coordinates and B(eq)[a]

atom	X/a	Y/b	Z/c	B(eq)*
Sb	0.46549 (7)	0.23426 (4)	0.01087 (3)	2.77 (2)
S	0.2704 (2)	0.0410 (2)	−0.0751 (1)	3.12 (6)
Cl	0.2437 (3)	0.4412 (2)	−0.0499 (1)	4.29 (8)
C(1)	0.414 (1)	0.0610 (7)	−0.1773 (4)	2.9 (2)
C(2)	0.326 (1)	0.1754 (8)	−0.2436 (4)	4.0 (3)
C(4)	0.706 (1)	0.1521 (9)	−0.2555 (4)	4.2 (3)
C(3)	0.511 (1)	0.225 (1)	−0.2991 (5)	5.0 (4)
C(6)	0.673 (1)	0.2436 (7)	−0.0991 (4)	3.1 (3)
C(5)	0.648 (1)	0.1090 (7)	−0.1610 (4)	3.1 (3)

[a] The number in parentheses in this and all subsequent tables is the estimated standard deviations in the least significant figure.

Table II. Intramolecular Distances (Å)

Sb–C(6)	2.156 (6)	C(5)–C(4)	1.528 (9)
Sb–S(1)	2.441 (2)	C(5)–C(1)	1.551 (8)
Sb–Cl(1)	2.454 (2)	C(1)–C(2)	1.507 (9)
S(1)–C(1)	1.827 (6)	C(2)–C(3)	1.53 (1)
C(6)–C(5)	1.511 (8)	C(4)–C(3)	1.51 (1)

Table III. Intramolecular Bond Angles (deg)

C(6)–Sb–S(1)	86.2 (2)	C(4)–C(5)–C(1)	100.6 (5)
C(6)–Sb–Cl(1)	92.6 (2)	C(2)–C(1)–C(5)	104.2 (5)
S(1)–Sb–Cl(1)	93.10 (6)	C(2)–C(1)–S(1)	115.8 (5)
C(1)–S(1)–Sb	96.7 (2)	C(5)–C(1)–S(1)	113.7 (4)
C(5)–C(6)–Sb	113.0 (4)	C(1)–C(2)–C(3)	106.4 (6)
C(6)–C(5)–C(4)	110.8 (5)	C(3)–C(4)–C(5)	106.7 (5)
C(6)–C(5)–C(1)	112.6 (5)	C(4)–C(3)–C(2)	105.6 (6)

Compound 10b. Yield 0.236 g, 0.87 mmol, 58%. Mp 117–124 °C dec. ^{1}H NMR (300 MHz, C_6D_6) δ 4.10 (dd, J = 4.7, 2.3 Hz, 1 H), 3.13 (m, 1 H), 1.95 (m, 3 H), 1.75 (m, 2 H), 1.31 (m, 1 H), 1.27 (m, 2 H). $^{13}C\{^1H\}$ NMR (75.4 MHz, $CDCl_3$) δ 63.93, 53.56, 46.13, 34.79, 31.25, 23.38. IR (KBr) 2969, 2950, 2862, 1468, 1398, 1300, 1256, 1130, 932, 721. HRMS Calcd for $C_6H_{10}SSbCl$: 269.9229. Found: 269.9234 ± 0.0006 amu.

Crossover Experiments. The following is a representative crossover experiment. Compound **3b** (15 mg, 0.06 mmol) was dissolved in 350 μL of C_6D_6 in an NMR tube and the tube was sealed with a septa and brought out of the drybox. A benzene-d_6 solution of compound **4b** (25 mg, 0.06 mmol, in 300 μL) was added to the tube via syringe. ^{1}H and ^{13}C NMR spectra were acquired and found to be identicle with those of authentic mixtures of the four compounds (**3b**,**c**, **4b**,**c**); however, resonances for the individual species could not be assigned in either sample. The contents of the tube was transferred to a schlenk flask and the solvent removed in vacuo to yield a white solid. The material was stored under argon for 27 h at room temperature and then analyzed by unit resolution mass spectrometry at ambient temperature. All four compounds were found to be present in equal amounts on the basis of the intensities of parent ions. Subsequent experiments indicated the results were independent of the time (≥5 min required) the mixture was allowed to stand, either in solution or as a solid. Control reactions in which the compounds were mixed as solids and analyzed as above indicated ≤10% crossover occurs on analysis.

Crystallography for 10b. Data Collection. A clear prism of $C_6H_{10}S$-SbCl having approximate dimensions of 0.150 × 0.150 × 0.150 mm was mounted on a glass fiber. All measurements were made on an Enraf-Nonius CAD-4 diffractometer with graphite monochromated Mo Kα radiation.

Cell constants and an orientation matrix for data collection, obtained from a least-squares refinement with the setting angles of 25 carefully centered reflections, corresponded to a monoclinic cell with dimensions a = 6.3319 (6) Å, b = 8.8161 (6) Å, c = 15.015 (2) Å, β = 95.504 (1)°, V = 837.4 (3) Å^3. For Z = 4 and fw = 271.41, the calculated density is 2.153 g/cm^3. On the basis of the systematic absences of $h0l$ ($h + l \neq 2n$) and $0k0$ ($k \neq 2n$) and the successful solution and refinement of the structure, the space group was determined to be $P2_1/n$ (No. 14).

The data were collected at a temperature of 23 ± 1 °C with use of the ω scan technique to a maximum 2θ value of 54.9°. ω scans of several intense reflections, made prior to data collection, had an average width at half-height of 0.37° with a take-off angle of 2.8°. Scans of (1.10 + 0.35 tan θ)° were made at speeds ranging from 1.8 to 16 deg/min (in ω). Moving-crystal moving counter background measurements were made by scanning an additional 25% above and below the scan range. The counter aperture consisted of a variable horizontal slit with a width

Table IV. Intermolecular Distances (Å)

	distance	ADC
Sb–S(1)	3.078 (2)	65503
Sb–Cl(1)	3.439 (2)	66503
Sb–C(1)	3.665 (6)	65503
	(Contacts to 3.8 Å)	

Table V. Experimental Details

A. Crystal Data	
empirical formula	$C_6H_{10}SSbCl$
formula weight	241.41
cryst color, habit	white, prism
crystal dimns, mm	0.200 × 0.180 × 0.150
crystal system	monoclinic
no. of reflcns used for unit cell determination (2θ range)	25 (25.0–35.0°)
ω scan peak width at half-height	0.37
lattice parameters	
a, Å	6.3319 (6)
b, Å	8.8161 (6)
c, Å	15.015 (2)
β, deg	95.504 (1)
V, Å^3	837.4 (3)
space group	$P2_1/n$ (No. 14)
Z	4
D_{calc}, g/cm^3	2.153
F_{000}	520
μ(Mo Kα), cm^{-1}	37.93
B. Intensity Measurements	
diffractometer	Enraf–Nonius CAD-4
radiation	Mo Kα(λ = 0.71069 Å)
temp, °C	23
attenuator	Zr foil (factor = 17.9)
take-off angle, deg	2.8
detector aperture, mm	3.0–3.5 horizontal, 4.0 vertical
cryst to detector dist	17.3
scan type	ω–2θ
scan rate, min^{-1}	1.1–16.0 (in ω)
scan width, deg	(1.10 + 0.35 tan θ)
2θ_{max}, deg	54.9
total no. of reflcns measd	228
no. of unique reflcns	2049 (R_{int} = 0.039)
corrections	Lorentz–polarization absorption (trans. factors: 0.94–1.11) secondary extinction (coeff = 0.39610 × 10^7)
C. Structure Solution and Refinement	
structure soln	Patterson method
hydrogen atom treatment	included in calcd positions (d_{C-H} = 0.96 Å)
refinement	full-matrix least-squares
function minimized	$\sum w(\lvert F_o\rvert - \lvert F_c\rvert)^2$
least-squares weights	$4Fo^2/\sigma^2(Fo^2)$
p factor	0.03
anomalous dispersion	all non-hydrogen atoms
no. of observations ($I > 3.00s(I)$)	1374
no. of variables	83
reflcn/parameter ratio	16.55
residuals: R; Rw	0.033; 0.037
goodness of fit indicator	1.09
max shift/error in final cycle	0.00
max peak in final diff map, e^{-1}/Å^3	0.50
min peak in final diff map, e^{-1}/Å^3	−1.06

ranging from 3.0 to 3.5 mm and a vertical slit set to 4.0 mm. The diameter of the incident beam collimator was 0.8 mm and the crystal-to-detector distance was 17.3 cm. For intense reflections an attenuator (attenuation factor = 17.93) was automatically inserted in front of the detector.

Data Reduction. Of the 2228 reflections that were collected, 2049 were unique (R_{int} = 0.040); equivalent reflections were merged. The intensities of three representative reflections that were measured after every 60 min of X-ray exposure time remained constant throughout data collection indicating crystal and electronic stability (no decay correction was applied). The linear absorption coefficient for Mo Kα is 37.9 cm^{-1}. An empirical absorption correction, using the program DIFABS,[12] was applied which resulted in transmission factors ranging from 0.83 to 1.11. The data were corrected for Lorentz and polarization effects. A correction for secondary extinction was applied (coefficient = 0.3691 × 10^{-07}).

Structure Solution and Refinement. The structure was solved by the Patterson method. The non-hydrogen atoms were refined anisotropically. Hydrogen atoms were included in the structure factor calculation in idealized positions (d_{C-H} = 0.95 Å) and were assigned isotropic thermal parameters that were 20% greater than the B_{eq} value of the atom to which they were bonded. The final cycle of full-matrix least-squares refinement[13] was based on 1374 observed reflections for which $I > 3.00s(I)$ and 83 variable parameters, and it converged (largest parameter shift was 0.00 times its esd) with unweighted and weighted agreement factors of

$$R = \sum\lvert\lvert F_o\rvert - \lvert F_c\rvert\rvert/\sum\lvert F_o\rvert = 0.033$$

$$R_w = [(\sum w(\lvert F_o\rvert - \lvert F_c\rvert)^2/\sum wF_o^2)]^{1/2} = 0.037$$

The standard deviation of an observation of unit weight[14] was 1.09. The weighting scheme was based on counting statistics and included a factor (ρ = 0.02) to downweight the intense reflections. Plots of $\sum w(\lvert F_o\rvert - \lvert F_c\rvert)^2$ versus $\lvert F_o\rvert$, reflection order in data collection, sin θ/λ, and various classes of indices showed no unusual trends. The final difference Fourier map was essentially featureless containing maximum and minimum peaks that corresponded to 0.50 and −1.06 e$^-$/Å^3, respectively.

Neutral atom scattering factors were taken from Cromer and Waber.[15] Anomalous dispersion effects were included in F_{calc}; the values for $\Delta f'$ and $\Delta f''$ were those of Cromer.[17] All calculations were performed with the TEXSAN crystallographic software package of Molecular Structure Corporation.[18]

Table V contains experimental details.

Acknowledgment. This work was supported, in part, by the Office of Naval Research and the donors of the Petroleum Research Fund, administered by the American Chemical Society, who we gratefully acknowledge. S.L.B. is a Fellow of the Alfred P. Sloan Foundation (1988–90), a Camille & Henry Dreyfus Teacher-Scholar (1988–93), an American Cancer Society Junior Faculty Research Awardee (1987–89), an Eli Lilly Grantee (1988–89), and an awardee of the Union Carbide Innovation Recognition Program (1988, 89). R.B.N. thanks the National Science Foundation for a Predoctoral Fellowship. We thank the U.S. Department of Energy (Grant No. DE-FG05-86ER-75292) for funding for the Rigaku AFC6R.

Supplementary Material Available: Tables of final observed and calculated structure factors for **10b** (13 pages). Ordering information is given on any current masthead page.

---

(12) DIFABS: Walker, Stuart, *Acta Crystallogr.* **1983**, *A39*, 158–166.

(13) Least-squares—function minimized, $\sum w(\lvert F_o\rvert - \lvert F_c\rvert)^2$, where $w = 4F_o^2/\sigma^2(F_o)$, $\sigma^2(F_o^2) = [S^2(C + R^2 + B) + (\rho F_o^2)^2]/Lp^2$, S = scan rate, C = total integrated peak count, R = ratio of scan time to background counting time, B = total background count, Lp = Lorentz–polarization factor, and ρ = ρ factor.

(14) Standard deviation of an observation of unit weight: $[\sum w(\lvert F_o\rvert - \lvert F_c\rvert)^2/(N_o - N_v)]^{1/2}$, where N_o = number of observations and N_v = number of variables.

(15) Cromer, D. T.; Waber, J. T. *International Tables for X-ray Crystallography*; The Kynoch Press: Birmingham, England, 1974; Vol. IV, Table 2.2 A.

(16) Ibers, J. A.; Hamilton, W. C. *Acta Crystallogr.* **1964**, *17*, 781.

(17) Cromer, D. T. *International Tables for X-ray Crystallography*; The Kynoch Press: Birmingham, England, 1974; Vol. IV, Table 2.3.1.

(18) TEXSAN–TEXRAY Structure Analysis Package, Molecular Structure Corporation, 1985.